



# Characterization of mullite in silicoaluminous fly ash by XRD, TEM, and $^{29}\text{Si}$ MAS NMR

S. Gomes\*, M. François

*Laboratoire de Chimie du Solide Minéral, UMR CNRS 7555, Université Henri Poincaré, Nancy, BP 239, 54506 Vandoeuvre Cedex, France*

Received 4 December 1998; accepted 25 October 1999

## Abstract

Mullite contained in a silicoaluminous fly ash (originating from power plant of La Maxe, near Metz in the east of France) issued from bituminous coal combustion has been studied by X-ray diffraction, nuclear magnetic resonance of  $^{29}\text{Si}$  spinning at magic angle, and transmission electron microscopy linked with energy-dispersive spectroscopy. By using results from X-ray diffraction [1] and nuclear magnetic resonance spectroscopy [2], an average value of 0.35 for  $x$ , the oxygen holes rate in mullite  $\text{Al}_{4+2x}\text{Si}_{2-2x}\text{O}_{10-x}$ , could be determined. Thus,  $\text{Al}_2\text{O}_3$  content is only slightly higher than those corresponding to the classical formula  $(\text{Al}_2\text{O}_3)_3 \cdot (\text{SiO}_2)_2$ . It is shown also that the composition is heterogeneous and depends on the crystallites; Ti and Fe are impurities substituting for Al in the structure. The average chemical formula of the mullite determined here is  $\text{Al}_{4.61}\text{Fe}_{0.05}\text{Ti}_{0.02}\text{O}_{9.65}$ . © 2000 Elsevier Science Ltd. All rights reserved.

**Keywords:** Fly ash; Characterization; X-ray diffraction; TEM; Mullite

## 1. Introduction

Mineralogical properties of silicoaluminous fly ashes, material removed from coal power plants, are well known [3–14]. Their composition depends on the nature of the coal source, which can contain more or less calcium oxide. A bituminous coal usually gives rise to class F material (i.e., with low-calcium content). Typically it consists of the crystallized phases  $\alpha$ -quartz, mullite, hematite, and magnetite in a matrix of aluminosilicate glass.

A question that has never been studied is the true chemical composition linked to the structural properties of mullite and magnetite in such residue, usually designed by their classical chemical formula  $(\text{Al}_2\text{O}_3)_3 \cdot (\text{SiO}_2)_2$  and  $\text{Fe}_3\text{O}_4$ , respectively. Indeed, contrary to  $\alpha$ -quartz, mullite and magnetite are nonstoichiometric compounds that can incorporate impurities. In this work, we were interested in studying mullite especially. Another paper concerns magnetite contained in a silicoaluminous fly ash [15].

Attempts to link mullite composition with other parameters such as the working temperature in the furnace of the power of the plant, the source coal, and the mineralogical composition of the fly ash could be made. For example, if a correlation between mullite composition and working temperature of the power plant exists, it could be used as an in-

dicator of the thermal history of the ash, which probably influences its pozzolanic reactivity.

It has been shown that both X-ray diffraction (XRD) [1] and nuclear magnetic resonance (NMR) techniques [2] can be employed efficiently to measure the value of  $x$ , the oxygen hole rate in a mullite of general formula  $\text{Al}_{4+2x}\text{Si}_{2-2x}\text{O}_{10-x}$ , and thus to approach the mullite composition. These works concerned synthetic mullite prepared from elementary oxides. It was interesting to apply these techniques to mullite contained in a silicoaluminous fly ash. Thus, composition of such mullite is determined by these methods and additionally by transmission electron microscopy (TEM) linked with energy-dispersive spectroscopy (EDS) analysis. The results are compared and discussed.

### 1.1. Composition and lattice parameters

Mullite crystallizes in a solid solution [16] with a homogeneity domain situated between 71 and 74 wt% of  $\text{Al}_2\text{O}_3$ . Its crystallographic structure is well known and is redrawn in Fig. 1 from structural data found in Ban and Okada [17]. It can be considered a sillimanite derivative with disordered hole oxygen atoms, corresponding to the general formula:  $\text{Al}_{4+2x}\text{Si}_{2-2x}\text{O}_{10-x}$ , where  $x$  is the number of oxygen holes per formula unit. The mechanism leading to the formation of one oxygen hole is due to the substitution of two silicon by two aluminum atoms:  $\text{O}^{2-} + 2\text{Si}^{4+} \rightarrow 2\text{Al}^{3+} + \square$ . Sillimanite corresponds to  $x$  equal zero. The mullite structure is usually described by  $\text{AlO}_6$  edges sharing octahedra that

\* Corresponding author. Tel.: +33-3-83-91-24-99; fax: +33-3-83-91-21-66.

E-mail address: sandrine.gomes@lcsm.v-nancy.fr

form parallel chains along [001] direction. These chains are connected by double chains of  $\text{TO}_4$  tetrahedra, also parallel to [001], where T can be Si or Al atoms. In the sillimanite structure, tetrahedra  $\text{TO}_4$  are alternatively centered by Si and Al atoms along [001] leading to a  $c$  parameter twice those of mullite. In the mullite structure, because of oxygen holes, the arrangement of tetrahedra is more complex. Holes are formed where oxygen atoms connect  $\text{TO}_4$  tetrahedra (site Oc on the drawing). Thus, to keep a fourfold coordination, Al-atoms move toward neighboring O-atoms (called Oc\*), leading to the formation of (T,T,T\*) tricluster. It has been shown that Si atoms occupy the T site only [18].

As is usual in a solid solution, lattice parameters strongly depend on the composition. The variation of the lattice parameters of the mullite as a function of the oxygen hole number  $x$  per formula unit was reported by Cameron [1]. It was shown that the  $a$  parameter presents the most significant variation and it was suggested it be used for determining the composition of any mullite.

It is also worth pointing out the existence of an alumina-rich mullite with composition  $\text{Al}_{5.65}\text{Si}_{0.35}\text{O}_{0.9.175}$  [19]. Its great number of oxygen holes leads to the formation of tetra clusters  $\text{T}_4\text{O}$ . So, it would be interesting to know if such mullite is encountered in silicoaluminous fly ash.

### 1.2. Composition and $^{29}\text{Si}$ MAS NMR spectrum

Nuclear magnetic resonance of  $^{29}\text{Si}$  spinning at magic angle has been used on synthetic mullite with various compositions [2]. This technique is sensitive to the local Si environment. It has been shown that the mullite structure con-

tains four NMR silicon sites (numbered from 1 to 4) and distinguished by the second neighbors, the first neighbor being always the four oxygen atoms of the tetrahedra. Site 1 (chemical shift  $\delta = -81$  ppm) corresponds to the silicon site near oxygen holes; site 2 ( $\delta = -86$  ppm) corresponds to a sillimanite site (i.e., a silicon tetrahedra surrounding by two adjacent  $\text{AlO}_6$  octahedra and three  $\text{AlO}_4$  tetrahedra); site 3 ( $\delta = -90$  ppm), so displaced by  $-4$  ppm compared to sillimanite site (site 2); and site 4 ( $\delta = -94$  ppm) shifted by  $-4$  ppm from site 3, corresponds to substitution of an Al-atom by an Si-atom in the second coordination sphere, so each  $\text{SiO}_4$  tetrahedron is surrounded in that case by two  $\text{AlO}_6$  octahedra, by only one  $\text{AlO}_4$  tetrahedra and thus by two  $\text{SiO}_4$  tetrahedra.

NMR spectra have been recorded as a function of the composition. The intensity of each NMR peak is proportional to the number of silicon in the corresponding sites; it has been shown (see Fig. 2) that their occupancy factors vary with composition and consequently with the number of oxygen hole per formula unit. Occupancy factor of site 1 (near oxygen holes) decreases linearly with  $2 \cdot x$  as the oxygen hole is accompanied by substitution of two Si-atoms by Al-atoms. Occupancy factor of site 2 and 3 decrease with  $1 \cdot x$ , those of site 4 are weakly occupied and approximately constant (its variation as a function of  $x$  is not so significant).

The fly ash used here originated from bituminous coal, which contains about 0.9 wt% of sulfur (originated from La Maxe's power plant, near Metz in the east of France). Its mineralogical composition determined by quantitative X-ray diffraction (QXRD) analyses is typical of class F [20]: mullite ( $\text{Al}_6\text{Si}_2\text{O}_{13}$ ) 25 wt%,  $\alpha$  quartz ( $\alpha\text{-SiO}_2$ ) 9 wt%, magnetite ( $\text{Fe}_3\text{O}_4$ ) 4 wt%, hematite ( $\text{Fe}_2\text{O}_3$ ) < 1 wt%, and 62 wt% of a silicoaluminous vitreous phase. It is shown that mullite is mainly formed during the coal combustion from kaolinite ( $\text{Al}_2\text{Si}_2\text{O}_5(\text{OH})_4$ ) [21], a clay mineral present as an impurity in the coal source.

The aim of this work is to complete the characterization of the mullite contained in a silicoaluminous fly ash. For this purpose, mullite is first extracted from the coal residues and then analyzed by XRD, its composition determined by chemical analysis (EDS) linked with TEM observations and NMR spectra recorded, and compared to earlier results described above and used as reference.

## 2. Experimental procedure

### 2.1. Mullite extraction from the silicoaluminous fly ash

The method used to extract the mullite from a silicoaluminous fly ash is prompted from a previous work [22]. It consists of dissolving vitreous phase in which mullite is embedded by dilute fluoride acid. Cenospheres are used preferentially to the whole part of silicoaluminous fly ash because they contain less iron oxides. Indeed, magnetite has undesirable effects on NMR spectra. Our separation method can be described by three steps:

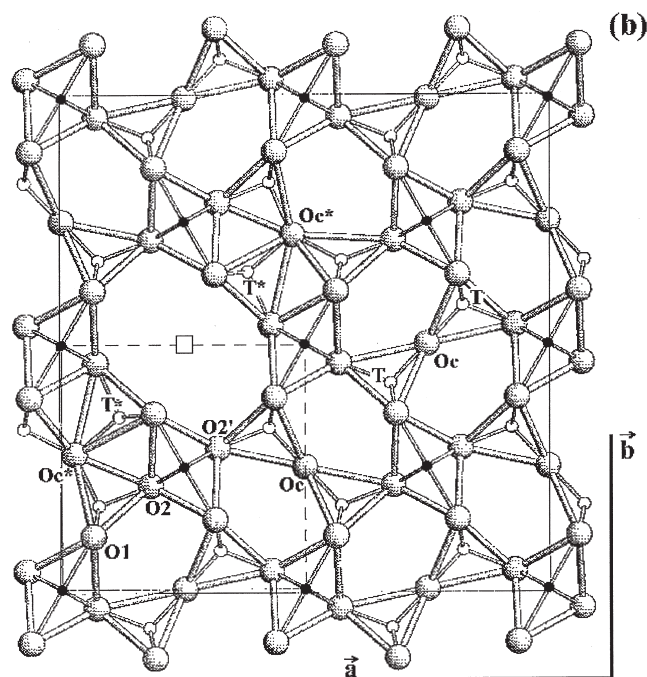


Fig. 1. Projection of the mullite structure along [001], from crystallographic data found elsewhere [17]. It shows the coordination geometry of the cations.

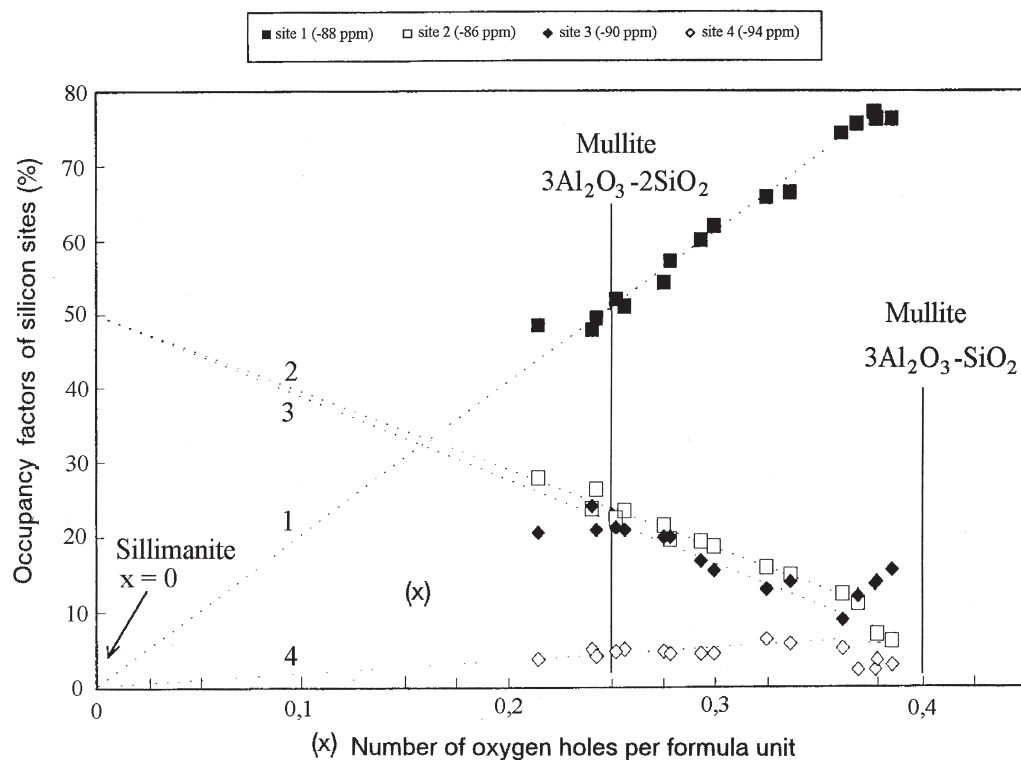


Fig. 2. Variations of the occupancies of the four different sites with the number oxygen holes per formula unit, copied from Fig. 4 of Jaymes et al. [2]. These curves are used as standard for interpreting our NMR results.

Step 1 (magnetite separation): cenospheres are finely grinded, put in water, and magnetically shaken. Iron oxides are naturally fixed on the permanent magnet and so can be easily removed. Powder is dried after filtration and verified by magnetic susceptibility measurements.

Step 2 (dissolution by dilute fluorhydric acid): the obtained powder (100 mg) after step 1 is mixed with fluorhydric dilute acid solution (2.5 mL) at 3% in a plastic bottle. The solution is then decanted after 15 h.

Step 3 (extraction): the solid part is washed with a great quantity of water, and successively by dilute HCl (4N), dilute HNO<sub>3</sub> (4N), and by ethyl diamine tetra acid (EDTA) at pH 7 then at pH 9. This step is repeated several time. The remaining powder is then weighted. The weight loss (≈70 wt%) corresponds to the proportion of vitreous phase and a majority of α-quartz contained in this silicoaluminous fly ash. The extracted mullite is then checked by XRD, scanning electron microscopy (SEM) observations and susceptibility measurements.

## 2.2. XRD

Powder patterns have been recorded by using a powder diffractometer (Inel, Artenay, France) with Bragg-Brentano geometry, equipped with a Molybdenum tube (quartz

monochromator, Kα<sub>1</sub> radiation, λ = 0.70930 Å). The lattice parameter are refined from the position of 40 corrected Bragg peaks (silicon is used as internal standard) by using UFIT program [23].

## 2.3. TEM and EDS analysis

TEM (Philips CM20 [Limeil Brévannes, France] operating at 200 kV and equipped with an energy dispersive spectrometer) is used to determine the chemical composition of the crystallites of mullite. The mullite is simply ground and hung in absolute alcohol. Then, one droplet of the mixture is deposited on a conductive sample grid. Some electronic diffraction pattern are realised on mullite needles for verification. Chemical analysis (EDS) is made by using Albite (NaAlSi<sub>3</sub>O<sub>8</sub>) as internal standard for Al and Si elements.

## 2.4. <sup>29</sup>Si MAS NMR

The experiment was performed on a Bruker MSL-300 spectrometer (Wissembourg, France), operating at a magnetic field strength of 7.0 Tesla. The sample was put in zirconia rotors, spinning at the magic angle of 54°44' at 4 kHz, using a pulse length of 4.5 μs and a recycle time of 15 s. About 10,000 scans were necessary to obtain a correct signal. The chemical shifts are referenced to tetramethylsilane. The NMR peaks are fitted by Gaussian lines. The variation

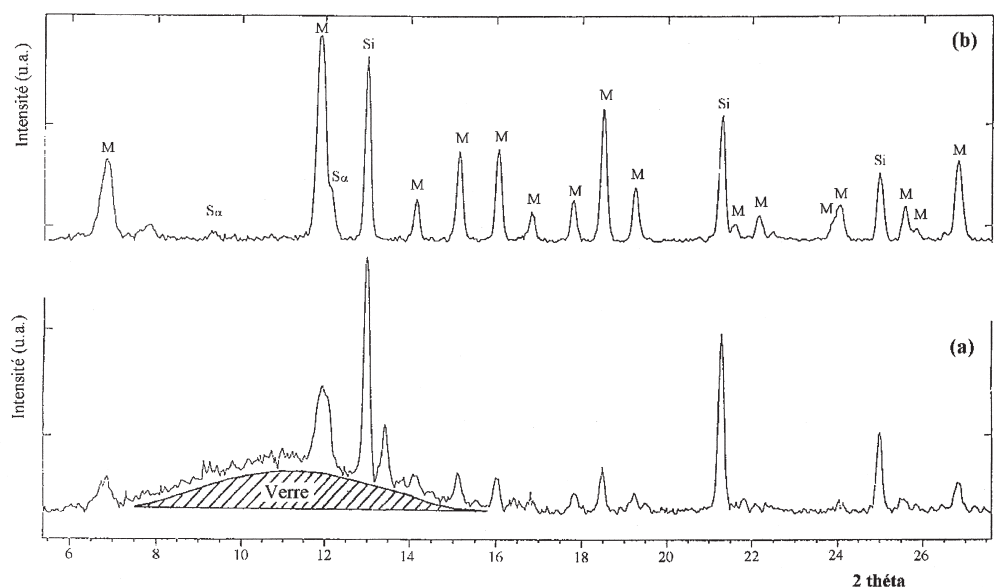


Fig. 3. XRD patterns ( $\lambda = 0.70930 \text{ \AA}$ ) of the silicoaluminous fly ash (cenosphere part only) (a) before treatment and (b) after treatment with dilute HF. M = mullite,  $S\alpha$  = alpha quartz. Si is used as internal standard.

of their intensity as a function of the hole composition exposed in another work [2] is reported in Fig. 2 and is used as reference.

### 3. Results and discussion

#### 3.1. XRD

The pattern before and after the treatment with dilute HF is shown in Figs. 3a and b, respectively. The disappearance of the vitreous phase is clearly seen, and the remaining phase is mullite with a small amount of  $\alpha$ -quartz. The lattice parameters,  $a = 7.557(4) \text{ \AA}$ ,  $b = 7.675(4) \text{ \AA}$ , and  $c = 2.882(1) \text{ \AA}$  are refined with a correct reliability factor of 3.7%. For comparison, those of mullite corresponding to ASTM no. 15-0776 card are  $a = 7.5456 \text{ \AA}$ ,  $b = 7.6898 \text{ \AA}$ , and  $c = 2.8842 \text{ \AA}$ .

#### 3.2. Orthorhombicity

An orthorhombicity parameter, defined as  $100 \times (b - a) / (b + a)$ , has been calculated from the curve given elsewhere [1], showing the variation of lattice parameters as a function of the hole concentration  $x$ . The variation of orthorhombicity as a function of  $x$  is reported in Fig. 4. The linear variation shows that the relaxation induced by formation of holes affects the basis (a,b) planes of the mullite. So, it is worth taking advantage of the fact that this relative parameter is free of zero shift error that can occur in lattice parameter measurements. The orthorhombicity of 0.77(5)%, measured on our sample, corresponds to an  $x$  value of 0.35(2) and a

composition of  $\text{Al}_{4.70}\text{Si}_{1.30}\text{O}_{9.65}$  or to a mullite with 75.5 wt% of  $\text{Al}_2\text{O}_3$ . It can be deduced from these XRD results that mullite contained in this silicoaluminous fly ash has a classical composition, only slightly more enriched with  $\text{Al}_2\text{O}_3$  than those corresponding to  $(\text{Al}_2\text{O}_3)_3 \cdot (\text{SiO}_2)_2$ .

#### 3.3. $^{29}\text{Si}$ MAS NMR

Experimental and fitted NMR spectra are reported in Fig. 5. The simulated spectrum corresponds to the sum of the four Gaussian peaks noted from 1 to 4. The reliability factor between the experimental and simulated spectrum (sum of the four Gaussian lines) has a value of 2.5%. The position of their maximum corresponds to the values reported else-

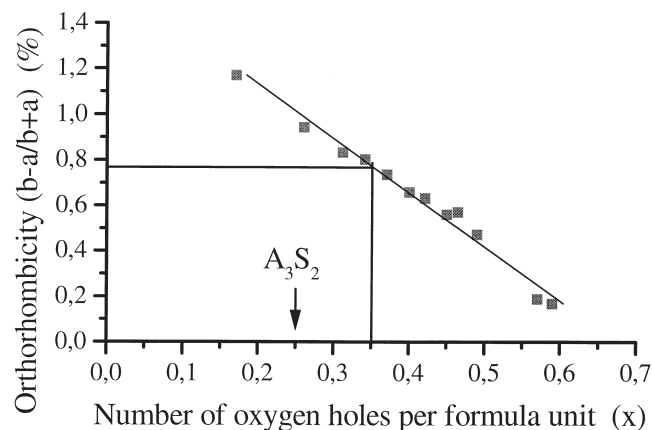


Fig. 4. Variation of the orthorhombicity as a function of oxygen vacancies content ( $x$ ) per formula unit in  $\text{Al}_{4+2x}\text{Si}_{2-2x}\text{O}_{10-x}$ , calculated from another work [1].  $A_3S_2$  = mullite.

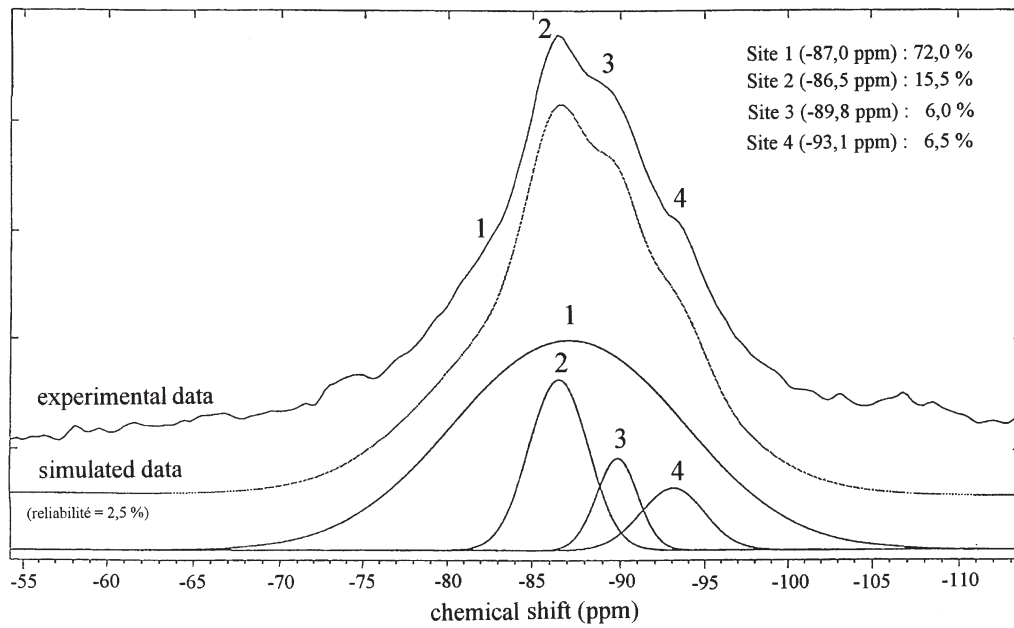


Fig. 5. Observed and calculated  $^{29}\text{Si}$  MAS NMR spectra of the mullite contained in the silicoaluminous fly ash.

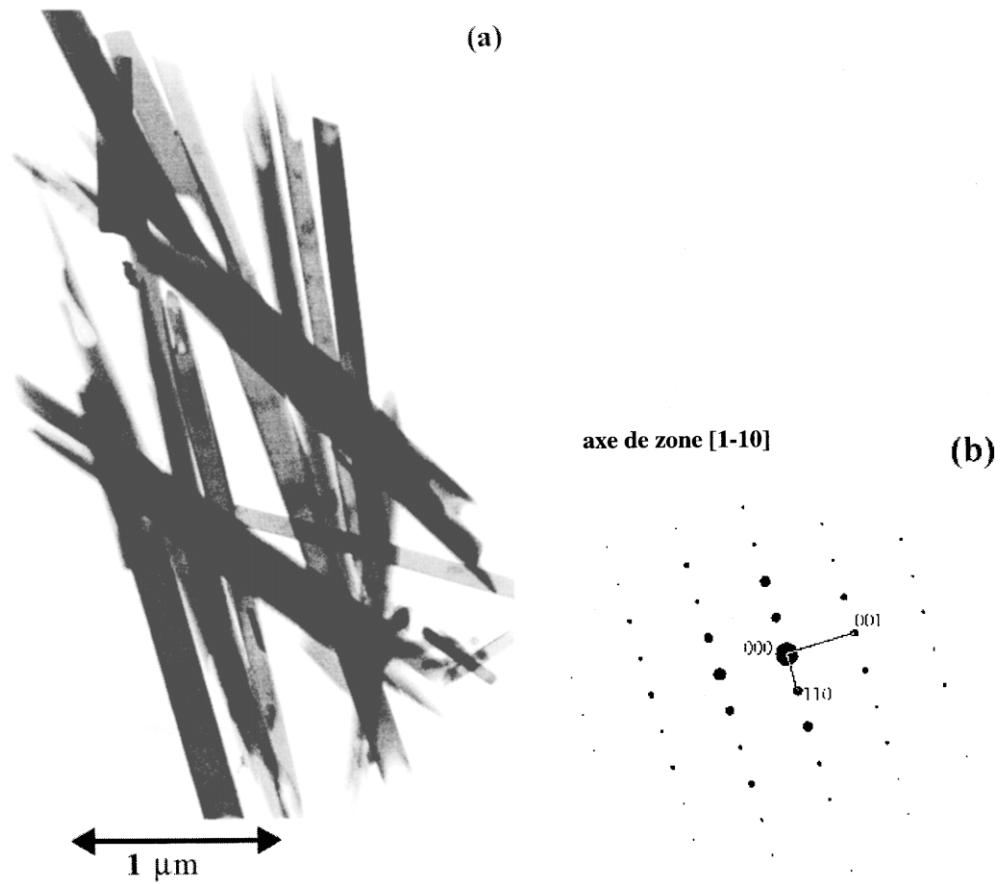


Fig. 6. TEM photograph of mullite needles (a) and electronic diffraction pattern (b) along [1-10] zone axis.

Table 1

Composition of mullite formed in silicoaluminous fly ash, expressed in the formula unit  $(\text{Al,Fe,Ti})_{4+2x}\text{Si}_{2-2x}\text{O}_{10-x}$

Points measured	Al	Si	Fe	Ti	Oxygen holes rate
1	4.300	1.336	0.350	0.015	0.332
2	4.780	1.189	0.023	0.009	0.406
3	4.304	1.330	0.348	0.018	0.335
4	4.805	1.180	0.003	0.012	0.410
5	4.810	1.176	0.004	0.010	0.412
6	4.715	1.260	0.007	0.017	0.370
7	4.753	1.219	0.008	0.020	0.390
8	4.796	1.175	0.007	0.022	0.413
9	4.764	1.214	0.000	0.022	0.393
10	4.813	1.143	0.013	0.030	0.428
11	4.735	1.212	0.025	0.027	0.394
12	4.683	1.294	0.014	0.009	0.353
13	4.658	1.2808	0.032	0.031	0.360
14	4.667	1.332	0.001	0.000	0.334
15	4.467	1.345	0.175	0.013	0.327
16	4.539	1.413	0.032	0.015	0.293
17	4.450	1.406	0.108	0.035	0.297
18	4.627	1.310	0.017	0.045	0.345
19	4.479	1.441	0.045	0.034	0.279
20	4.576	1.369	0.020	0.034	0.316
21	4.562	1.404	0.013	0.021	0.298
22	4.538	1.393	0.054	0.015	0.303
23	4.603	1.365	0.007	0.024	0.317
24	4.481	1.499	0.016	0.005	0.250
25	4.720	1.244	0.031	0.004	0.378
26	4.764	1.208	0.015	0.013	0.396
27	4.600	1.262	0.129	0.009	0.369
28a	4.547	1.429	0.002	0.022	0.285
28b	4.560	1.413	0.004	0.023	0.293
28c	4.587	1.385	0.004	0.023	0.307
28d	4.683	1.294	0.004	0.019	0.353
29a	4.563	1.367	0.052	0.018	0.316
29b	4.658	1.285	0.041	0.015	0.358
29c	4.683	1.247	0.050	0.019	0.377
29d	4.554	1.358	0.064	0.024	0.321
30a	4.582	1.334	0.068	0.016	0.333
30b	4.582	1.336	0.068	0.013	0.332
30c	4.606	1.312	0.066	0.016	0.344
30d	4.568	1.347	0.070	0.015	0.326
31a	4.423	1.409	0.154	0.013	0.295
31b	4.529	1.320	0.143	0.008	0.340
31c	4.552	1.345	0.097	0.006	0.328
31d	4.293	1.499	0.195	0.0122	0.250
32a	4.729	1.237	0.022	0.012	0.381
32b	4.782	1.189	0.019	0.009	0.406
32c	4.777	1.196	0.014	0.012	0.402
32d	4.658	1.320	0.012	0.010	0.340
33a	4.668	1.297	0.018	0.017	0.352
33b	4.688	1.278	0.019	0.014	0.361
33c	4.700	1.266	0.022	0.015	0.367
33d	4.711	1.244	0.030	0.015	0.378
34a	4.492	1.450	0.045	0.012	0.275
34b	4.552	1.411	0.027	0.009	0.294
34c	4.576	1.383	0.029	0.011	0.308
34d	4.539	1.428	0.020	0.012	0.286
35a	4.601	1.358	0.018	0.023	0.321
35b	4.600	1.363	0.019	0.017	0.318
35c	4.568	1.399	0.015	0.0177	0.301
35d	4.555	1.402	0.016	0.027	0.299

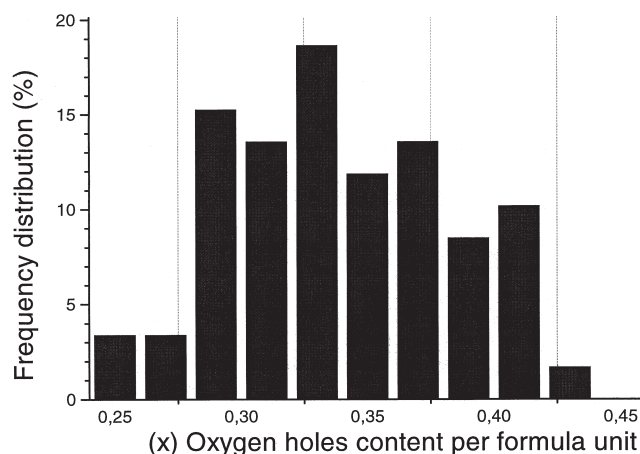


Fig. 7. Oxygen hole frequency distribution of the mullite contained in a silicoaluminous fly ash. Results are from analytical TEM analyses of 35 crystallites.

where [2]. The contribution of each silicon site and the corresponding  $x$  holes values deduced from Fig. 2 are inserted in the figure. The NMR  $x$  hole number found is 0.36(1), in good agreement with XRD results.

### 3.4. TEM analysis

Typical mullite crystallites with needlelike shape and corresponding electronic diffraction of zone axis [1-0] is reported in Fig. 6. The composition has been determined from 35 crystallites corresponding to 59 point measurements indicated in Table 1. It is expressed per formula unit  $\text{Al}_{4+2x}\text{Si}_{2-x}\text{O}_{10-x}$ , pointing out the  $x$  oxygen hole content. The results show the composition is heterogeneous from one crystallite to another but homogeneous in the same crystallite. The crystallites of mullite contain low quantities of Fe and Ti. A lower Al content corresponds always to a higher Fe content, meaning that  $\text{Al}^{3+}$  substitutes for  $\text{Fe}^{3+}$  cations in the mullite structure. Maximum values for Fe correspond to point 1 on the table (0.35/f.u.). It corresponds to substitution of 7.5% of Al by Fe atoms. Substitution of Al by Ti is less clear, but is probably the same case. Maximum value for Ti (0.023/f.u.) is measured on point 35d. It corresponds to substitution of 0.6% of Al by Ti atoms. The discrepancy of the composition of the  $x$  value is shown in Fig. 7, where the frequency distribution of the 59 points analyzed as a function of  $x$  is reported. The  $x$  values set in the range 0.25 to 0.45, with an average of 0.34(2), correspond in the accuracy of the measurements to X-ray and NMR results.

## 4. Conclusions

A value of 0.35 for  $x$ , the rate of oxygen holes in mullite  $\text{Al}_{4+2x}\text{Si}_{2-x}\text{O}_{10-x}$  contained in a silicoaluminous fly ash originated from coal combustion has been determined inde-



pendently by XRD measurements and  $^{29}\text{Si}$  NMR MAS spectroscopy. So, the alumina content determined in such mullite is only slightly higher compared to the classical formula  $\text{Al}_{4.5}\text{Si}_{1.5}\text{O}_{9.75}$ .

TEM coupled with EDS analyses is in agreement with this composition and brings supplementary information. Composition determined above is only an average on the analyzed sample. In fact, mullite of the ash is very heterogeneous. This is not surprising since the natural conditions involved by the fast cooling rate of the fume are not favorable for a good crystallization and homogenization. Mullite contains Fe as a main impurity, which can substitute for Al in the structure. A maximum of 7.5 at% of Fe and 0.6 at% of Ti substituting Al has also been detected.

Finally the average chemical formula  $\text{Al}_{4.61}\text{Fe}_{0.05}\text{Ti}_{0.02}\text{O}_{9.65}$  characterizes well the mullite contained in a sample of silicoaluminous fly ash studied here. It has been proven that an accurate measurement of the lattice parameters of the mullite contained in the ash is enough to have partial but available information on its average composition.

Characterization of mullite contained in the residues can be made easily by XRD and could be done on various fly ashes to observe similarities or differences following their origins.

## Acknowledgments

The author wishes to thank engineer of EDF (Electricité de France) C. Pellissier for the samples of fly ashes. The work described has been carried out as part of the research program of EDF and this paper is published with permission of C. Pellissier. TEM analyses were conducted by J. Ghanbaja from the Service Commun de Microscopie Electronique en Transmission, NMR measurements were conducted by P. Tekely and C. Malveau from the Service Commun de Résonance Magnétique Nucléaire from the Faculty of Sciences, Vandoeuvre les Nancy (France).

## References

- [1] W.E. Cameron, Mullite: A substituted alumina, *Am Mineral* 62 (1977) 747–755.
- [2] I. Jaymes, A. Douy, D. Massiot, J. P. Coutures, Evolution of the Si environment in mullite solid solution by  $^{29}\text{Si}$  MAS-NMR spectroscopy, *J Non-Crystallin Sol* 204 (1996) 125–134.
- [3] M. Regourd, in: 8th ICC, Rio de Janeiro, Brazil, Aba Gráfica e Editora, Vol. I, 1986, pp. 200–229.
- [4] F.M. Lea, *The Chemistry of Cement Concrete*, Edward Arnold Ltd, London, 1970.
- [5] H. Pietersen, A.L.A. Fraay, J. Bijen, Reactivity of fly ash at high pH, *Mat Res Soc Symp Proc* 178 (1990) 139–157.
- [6] J.C. Qian, E.E. Lachowski, F.P. Glasser, Microstructure and chemical variation in class F fly ash glass, *Mat Res Symp Proc* 113 (4) (1988) 45–53.
- [7] M. Venuat, *Adjuvants et Traitements*, M. Venuat, Paris, 1984.
- [8] J.C. Qian, E.E. Lachowski, F.P. Glasser, The microstructure of National Bureau of standards reference fly ashes, *Mat Res Soc Symp Proc* 136 (5) (1989) 77–85.
- [9] C.L. Kilgour, K.L. Bergeson, S. Schlorholtz, Storage alternatives for high-calcium fly ashes, *Mat Res Soc Symp Proc* 136 (5) (1989) 161–168.
- [10] M.M. Alasali, V.M. Malhotra, Role of concrete incorporating high volumes of fly ash in controlling expansion due to alkali-aggregate reaction, *ACI Mat J* 88 (2) (1991) 159–163.
- [11] S. Diamond, On the glass present in low-calcium and in high-calcium fly ashes, *Cem Concr Res* 13 (1983) 459–464.
- [12] G.J. McCarthy, D.M. Johansen, X-ray powder diffraction study of NBS fly ash standard reference materials, *Power Diffr* 3 (3) (1988) 156–161.
- [13] G.J. McCarthy, K.J. Solem, X-ray diffraction analysis of fly ash. II. Results, *Adv X-Ray Anal* 34 (1991) 387–394.
- [14] G.J. McCarthy, X-ray powder diffraction for studying the mineralogy of fly ash, *Mat Res Soc Proc* 113 (4) (1988) 75–86.
- [15] S. Gomes, M. François, M. Abdelmoula, C. Pellissier, O. Evrard, Characterisation of magnetite in silico-aluminous fly ash by SEM, TEM, XRD, magnetic susceptibility and Mössbauer spectroscopy, *Cem Con Res* 29 (1999) 1705–1711.
- [16] F.J. Klug, S. Prochazka, R.H. Doremus, Alumina-silica phase diagram in the mullite region, in: S. Somiya, R.F. Davis, J.A. Pask (Eds.), *Mullite and Mullite Matrix Composites*, Ceramic Transactions, Vol. 6, The American Ceramic Society, Westerville OH, 1990, pp. 15–41.
- [17] T. Ban, K. Okada, Structure refinement of mullite by the Rietveld method and a new method for estimation of chemical composition, *J Am Ceram Soc* 75 (1992) 227–230.
- [18] R.J. Angel, R.K. McMullan, C.T. Prewitt, Substructure and superstructure of mullite by neutron diffraction, *Am Mineral* 76 (1991) 332–342.
- [19] R.X. Fischer, H. Schneider, M. Schmücker, Crystal structure of Al-rich mullite, *Am Mineral* 79 (1994) 983–990.
- [20] S. Gomes, M. François, O. Evrard, C. Pellissier, Characterization and comparative study of coal combustion residues from a primary and additional flue gas secondary desulfurization, *Cem Concr Res* 28 (11) (1998) 1605–1619.
- [21] R.C.D. Slade, T.W. Davies, Evolution of structural changes during flash calcination of kaolinite—A  $^{29}\text{Si}$  and  $^{27}\text{Al}$  nuclear magnetic resonance spectroscopy study, *J Mater Chem* 1 (3) (1991) 361–364.
- [22] L.D. Hulett, A.J. Weinberger, Some etching studies of the microstructure and composition of large aluminosilicate particles in fly ash from coal-burning power plants, *Environ Sci Technol* 14 (8) (1980) 965–970.
- [23] M. Evain, *UFIT program V1.3*, Institut des Matériaux de Nantes, Nantes, France 1992.